Volume 17 | Number 10 | October 2015 | Pages 4693–4850

Green Chemistry

Cutting-edge research for a greener sustainable future

www.rsc.org/greenchem

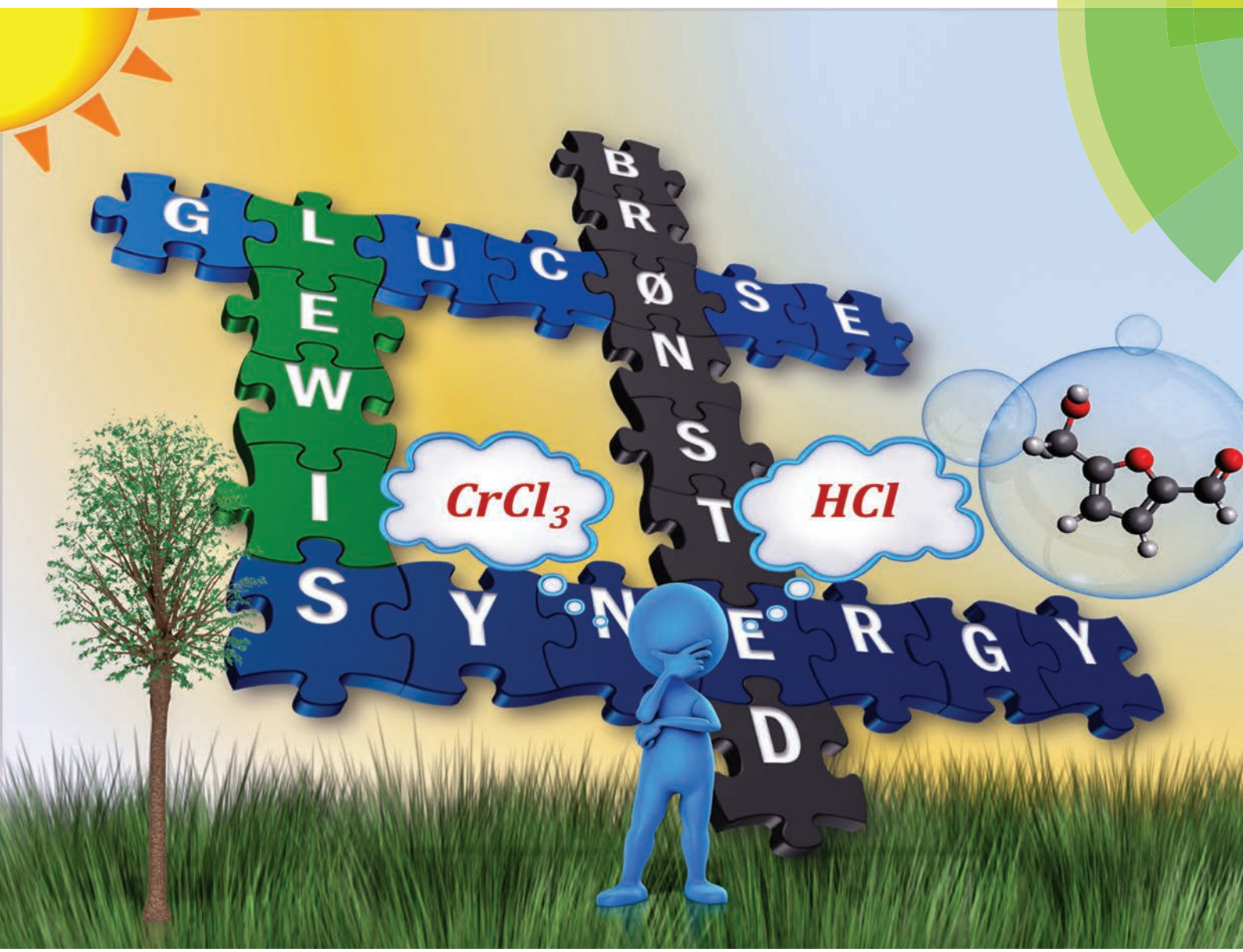

ISSN 1463-9262

ROYAL SOCIETY OF CHEMISTRY

PAPER

Vladimiros Nikolakis, Dionisios G. Vlachos *et al.*

Tandem Lewis/Brønsted homogeneous acid catalysis: conversion of glucose to 5-hydoxymethylfurfural in an aqueous chromium(III) chloride and hydrochloric acid solution

Green Chemistry

PAPER

View Article Online
View Journal | View Issue

Cite this: *Green Chem.*, 2015, **17**, 4725

Tandem Lewis/Brønsted homogeneous acid catalysis: conversion of glucose to 5-hydoxymethylfurfural in an aqueous chromium(III) chloride and hydrochloric acid solution†

T. Dallas Swift,[a] Hannah Nguyen,[a] Andrzej Anderko,[b] Vladimiros Nikolakis*[a] and Dionisios G. Vlachos*[a]

Received 8th June 2015,
Accepted 27th July 2015

DOI: 10.1039/c5gc01257k

www.rsc.org/greenchem

A kinetic model for the tandem conversion of glucose to 5-hydroxymethylfurfural (HMF) through fructose in aqueous $CrCl_3$–HCl solution was developed by analyzing experimental data. We show that the coupling of Lewis and Brønsted acids in a single pot overcomes equilibrium limitations of the glucose–fructose isomerization leading to high glucose conversions and identify conditions that maximize HMF yield. Adjusting the HCl/$CrCl_3$ concentration has a more pronounced effect on HMF yield at constant glucose conversion than that of temperature or $CrCl_3$ concentration. This is attributed to the interactions between HCl and $CrCl_3$ speciation in solution that leads to HMF yield being maximized at moderate HCl concentrations for each $CrCl_3$ concentration. This volcano-like behavior is accompanied with a change in the rate-limiting step from fructose dehydration to glucose isomerization as the concentration of the Brønsted acid increases. The maximum HMF yield in a single aqueous phase is only modest and appears independent of catalysts' concentrations as long as they are appropriately balanced. However, it can be further maximized in a biphasic system. Our findings are consistent with recent studies in other tandem reactions catalyzed by different catalysts.

Introduction

Recently, there has been an increased interest in the production of fuels and chemicals from renewably produced biomass derivatives. Glucose, the building block of cellulose, is an attractive feedstock since its furanic dehydration product, 5-hydroxymethylfurfural (HMF), is considered a very important platform chemical[1] as it can be upgraded in high selectivity to drop-in products like dimethyl furan,[2,3] *para*-xylene,[4] organic solvents,[5] *etc*. A main current barrier to commercialization includes the high cost, largely due to byproduct formation.[6,7] In addition, HMF is an unstable product and can easily decompose into levulinic acid and formic acid, or form polymeric compounds, especially in the presence of water.[7] Thus improving the conversion of glucose to HMF can have a significant impact on future biorefineries.

Unlike fructose, the Brønsted acid-catalyzed dehydration of glucose to HMF is slow.[8,9] It is then common to first isomerize glucose to fructose. This isomerization employs the largest industrial use of immobilized enzymes; over 10 million tons of glucose isomerase are produced annually for glucose to fructose isomerization.[10] Furthermore, it is an equilibrium-limited reaction, with an equilibrium constant of approximately unity[11] which unfortunately limits glucose conversion. To get around this limitation, Simeonov and coworkers have combined enzymatic isomerization of glucose to fructose in a first reactor with Brønsted acid catalyzed fructose dehydration to HMF in a second reactor[12] where fructose dehydrates to HMF and HMF is extracted to an organic phase, while the glucose is recycled to the isomerization reactor. This two-pot approach employs high glucose recycle to reach complete conversion and the operating range of the isomerization reactor is constrained from the sensitivity of the enzyme.

Lewis acids have been shown to be active for glucose–fructose isomerization,[13] and can also tolerate Brønsted acidity and high temperature, thus providing a promising alternative for the production of HMF from glucose in a single-pot.[14,15] The Davis group obtained HMF yields in excess of 50% in a one-pot reactor containing Lewis acidic Sn-Beta and HCl.[15] Following Davis' group pioneering work, many other tandem

[a]*Department of Chemical and Biomolecular Engineering, Catalysis Center for Energy Innovation, University of Delaware, 221 Academy Street, Newark, DE 19176, USA. E-mail: vlad@udel.edu, vlachos@udel.edu*
[b]*OLI Systems Inc., 240 Cedar Knolls Road, Suite 301, Cedar Knolls, NJ 07927, USA*
†Electronic supplementary information (ESI) available. See DOI: 10.1039/c5gc01257k

Lewis/Brønsted acid catalysts were investigated,[16] including aluminosilicate zeolites,[17] activated carbons,[18] and homogeneous metal chlorides,[19] such as $CrCl_3$ [14,20–23] and $AlCl_3$.[24] For the homogeneous Lewis acid $CrCl_3$/Brønsted acid HCl single pot catalysis, we revealed rather complex and unexpected interactions that render understanding experimentally challenging.[14]

The aim of the present work is to further understand the interactions of coupled Lewis and Brønsted acids in tandem reactions and specifically how to optimize the yield and rate of HMF. At the fundamental level, we are interested in understanding the kinetic regimes of tandem reactions catalyzed by different catalysts as these are commonplace in biomass processing. Toward this goal, we perform select experiments and develop the first skeleton model of coupled dual catalysts to acquire insights.

Methods

Reaction kinetics

A typical reaction was conducted in a sealed 5 mL thick walled glass vial, containing 2 mL aqueous solution of a reactant and a catalyst heated at desired reaction temperature. Reactants were fructose, mannose and HMF purchased from Sigma Aldrich and used a received. Catalysts were $CrCl_3 \cdot 6H_2O$ (Sigma Aldrich) and hydrochloric acid (Fisher Scientific). Details on the amounts of reactants and catalysts were listed on experiment 1–8 in Table 1. Kinetic study was performed by placing multiple glass reactors into a preheated aluminum reactor block (Chemglass) consisting on 17 wells, filled with mineral oil placed on a magnetic hot plate (Fisher Scientific) for control of temperature and stirring speed. Each well contained one reactor. At a specific time point, a reactor was taken out of the oil bath and immediately immersed in an ice bath to stop reaction.

Post reaction solutions, which contained brownish particles, were filtered with a 0.2 μm membrane nylon filter (Thermo Scientific) before being analyzed with high-performance liquid chromatography (HPLC – from Waters Alliance Instruments). Sugar compounds were detected by two Biorad HPX 87C columns in series heated to 75 °C, and HPLC grade water flowing at 0.5 mL min^{-1} was the mobile phase. Glucose, mannose and fructose eluted at 25, 29.5, and 32.7 minutes respectively. HMF, levulinic acid, and formic acid were detected by a Biorad HPX 87H column heated to 50 °C and 0.005 M sulfuric acid flowing at 0.5 mL min^{-1} was the mobile phase. HMF, levulinic acid, and formic acid eluted at 17, 19.6 and 38.3 minutes respectively. In the HPLC chromatograms, besides peak signals of glucose, fructose, mannose, HMF, levulinic acid and formic acid, other peaks were also observed indicating the formation of other soluble by-products. Most of these extra peak signals were only observed when reactants were sugars instead of HMF. Therefore, we believe that these by-products form *via* side reactions involving sugars or intermediates of them. In addition, since the area of these peaks

Table 1 Experimental conditions. Data are from this work unless otherwise stated

Experiment	Temperature (°C)	Substrate (wt%)	Catalyst	Ref.	Used for parameter estimation
1	110	Mannose (5)	5 mM $CrCl_3$		Yes
2	130	Mannose (5)	5 mM $CrCl_3$		Yes
3	110	Fructose (5)	5 mM $CrCl_3$		Yes
4	130	Fructose (5)	5 mM $CrCl_3$		Yes
5	110	HMF (5)	5 mM $CrCl_3$		Yes
6	130	HMF (5)	5 mM $CrCl_3$		Yes
7	110	Mannose (5)	45 mM HCl		Yes
8	130	Mannose (5)	45 mM HCl		Yes
9	130	Glucose (5)	5 mM $CrCl_3$		Yes
10	130	Glucose (5) + HMF (1.5)	5 mM $CrCl_3$		Yes
11	140	Fructose (10)	17 mM $CrCl_3$	14	Yes
12	150	Glucose (10)	17 mM $CrCl_3$	14	Yes
13	140	Glucose (10)	17 mM $CrCl_3$	14	Yes
14	130	Glucose (10)	17 mM $CrCl_3$	14	Yes
15	140	Glucose (10)	17 mM $CrCl_3$ + 0.1 M HCl	14	Yes
16	140	Fructose (10)	17 mM $CrCl_3$ + 0.1 M HCl	14	Yes
17	130	Glucose (1)	2 mM $CrCl_3$		No
18	150	Glucose (1)	2 mM $CrCl_3$		No
19	130	Glucose (5)	5 mM $CrCl_3$ + 5 mM HCl		No
20	130	Glucose (5)	5 mM $CrCl_3$ + 10 mM HCl		No
21	130	Glucose (5)	5 mM $CrCl_3$ + 34 mM HCl		No
22	130	Glucose (5)	5 mM $CrCl_3$ + 120 mM HCl		No
23	140	Glucose (10)	8.5 mM $CrCl_3$	14	No
24	140	Glucose (10)	25 mM $CrCl_3$	14	No
25	130	Glucose (5)	5 mM $CrCl_3$ + 0.01 M HCl		No
26	130	Glucose (5)	5 mM $CrCl_3$ + 0.1 M HCl		No
27	140	Glucose (10)[a]	17 mM $CrCl_3$ + 0.1 M HCl	14	No

[a] Biphasic reactor used (20 wt% NaCl in aqueous phase + 2 : 1 THF : H_2O).

was very small (less than 1% of the total HPLC area), quantification of these by-products was neglected in the reaction kinetic modelling study (no significant fractions of 5,5′-oxy(bismethylene)-2-furaldehyde were formed, consistent with the reaction being carried in water solvent).[25] Reactant conversion and yields of identified products were calculated as follows:

$$\text{Conversion}\,(\%) = \frac{c^{t=0}_{\text{reactant}} - c_{\text{reactant}}}{c^{t=0}_{\text{reactant}}} \times 100\%$$

$$\text{Yield}_i\,(\%) = \frac{c_i}{c^{t=0}_{\text{reactant}}} \times 100\%$$

where c_i is the concentration of species i.

A significant amount of carbon loss was accounted for by the formation of insoluble polymeric materials during the reaction, which were filtered out before the HPLC analysis. They are generally referred to as humins, formed from polymerization reactions of hexoses and HMF on either Brønsted acid or Lewis acid centers. The mechanism of humins formation as well as their structure have not yet been well determined and are subject to debate.[7] For our purposes, the humins' yield was estimated from the carbon balance of quantified products; thus it also accounts for the non-identified soluble products.

Experimental conditions

The experimental conditions, exploiting different temperatures, substrates, and catalyst concentrations, are listed in Table 1. Procedures of experiments conducted herein are reported in ref. 14. Experiments 1–16 were used for parameter estimation and experiments 17–27 were employed for model assessment.

Reaction network and kinetic modeling

We simulated the Brønsted acid chemistry using the reaction network shown with solid arrows in Scheme 1, leveraging previous work for reactions 1–5 [26,27] and 6–7 [28] whose temperature range and explicit pH dependence make them consistent with this work. Brønsted catalyzed mannose conversion to HMF and humins (reactions 8 and 9) have been quantified here for first time. The parameters of all Brønsted acid-catalyzed reaction rate laws are given in Table 2.

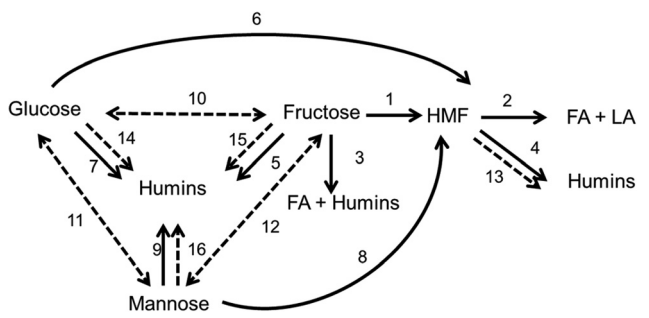

Scheme 1 Reaction network for tandem reaction of glucose conversion to HMF by $CrCl_3$ and HCl in aqueous phase.

A kinetic model for $CrCl_3$-catalyzed reactions has not yet been published. Building on the mechanistic insights proposed for glucose isomerization in Sn-BEA by the Davis group[29] and the reaction network of Rajabbeigi *et al.*,[30] we propose a Lewis acid catalyzed reaction network shown by dashed lines in Scheme 1 (reactions 10–16). The parameters of the Lewis acid-catalyzed reaction rate laws are also given in Table 1. The speciation of $CrCl_3$ in solution was calculated using the OLI Analyzer Studio version 9.2 (OLI Systems, 2012), which is based on the aqueous electrolyte model presented by Wang *et al.*[31] and was also used in our previous work.[14]

Parameter estimation involves fitting the transient profiles of glucose, mannose, fructose, HMF, and LA using the *fminunc* minimization routine in Matlab R2013a. A similar procedure for parameter estimation was previously employed for fructose dehydration kinetics in HCl.[26]

Results and discussion

Kinetic parameters

The reaction kinetics of Brønsted acid-catalyzed chemistry has been reported before, except for the Brønsted acid-catalyzed reactions of mannose. Thus, below we focus on the mannose chemistry in HCl and on the Lewis acid-catalyzed reactions.

Mannose conversion in HCl

Mannose dehydration is considerably less studied compared to that of glucose and fructose. Fig. 1 shows the experimental concentration profiles (points) and model predictions (lines) using the fitted parameters. HMF, FA/LA and humins are the main products, with humins being the most abundant. As noted by van Putten *et al.*, aldose sugars, including glucose and mannose, react similarly in aqueous solutions.[8] The estimated parameters of Brønsted catalyzed mannose dehydration to HMF are shown in Table 2. While no literature is available for direct comparison, the activation energy of mannose dehydration to HMF (175 kJ mol^{-1}) is similar to reported values of glucose dehydration to HMF (152–160 kJ mol^{-1}),[28,32] supporting the conclusion that mannose and glucose react similarly.[8] The activation energy for mannose degradation to humins (58 kJ mol^{-1}) is also consistent with the activation energy for glucose degradation to humins (51 kJ mol^{-1}).[28] As mannose is a minor product, no further experiments and model assessment were conducted.

HMF degradation in $CrCl_3$

The products and mechanisms of HMF degradation in aqueous $CrCl_3$ solutions have not yet been extensively studied. Fig. 2 shows the HMF conversion and carbon yield of LA, FA, and humins. At 110 °C, the yield to humins is much higher than that to either LA or FA. This differs significantly from Brønsted acid catalyzed chemistry, where the FA and LA account for over 80% of the HMF degradation products.[26] At 130 °C, the FA/LA yield is higher but humins remain the dominant product. The activation energies of Brønsted-acid

Table 2 Reactions, rate laws, and estimated parameters determined herein unless otherwise stated for reactions shown in Scheme 1. Parity plot for select experiments is shown in Fig. S3

Reaction	Catalyst	Rate expression	Activation energy, kJ mol^{-1}	$\ln(k_{403\ K}/\text{min}^{-1}\ \text{M}^{-1})$	$\log_{10}(A_0/\text{min}^{-1}\ \text{M}^{-1})$	Ref.
Glucose → fructose	$CrCl_3$	$k_i a_L C_{Glu}$	100 ± 5	−4.62 ± 0.03	11.0	[a]
Fructose → mannose	$CrCl_3$	$k_i a_L C_{Fru}$	91 ± 2	−5.44 ± 0.03	9.4	[a]
Mannose → glucose	$CrCl_3$	$k_i a_L C_{Man}$	80 ± 11	−6.08 ± 0.03	7.7	[a]
Fructose → humins	$CrCl_3$	$k_i a_L C_{Fru}$	114 ± 6	−5.33 ± 0.03	9.5	
Mannose → humins	$CrCl_3$	$k_i a_L C_{Man}$	68 ± 7	−5.43 ± 0.11	6.4	
Glucose → humins	$CrCl_3$	$k_i a_L C_{Glu}$	71 ± 19	−6.60 ± 0.10	6.4	
HMF → humins	$CrCl_3$	$k_i a_L C_{HMF}$	56 ± 9	−6.73 ± 0.11	4.2	
Mannose → HMF	HCl	$k_i C_H^+ C_{Man}$	175 ± 3	−4.98 ± 0.02	20.5	
Mannose → humins	HCl	$k_i C_H^+ C_{Man}$	58 ± 12	−4.45 ± 0.13	5.6	
Fructose → HMF	HCl	$k_i \phi_f \frac{C_{H^+}}{C_{H_2O}} C_{Fru}$	127 ± 2	1.44 ± 0.04[b]	18.1[c]	26, 27
Fructose → humins	HCl	$k_i C_H^+ C_{Fru}$	133 ± 7	−4.22 ± 0.16[b]	16.4	26, 27
HMF → FA/LA	HCl	$k_i C_H^+ C_{HMF}$	97 ± 1	−3.25 ± 0.02[b]	11.9	26, 27
HMF → humins	HCl	$k_i C_H^+ C_{HMF}$	64 ± 8	−5.14 ± 0.21[b]	6.6	26, 27
Fructose → FA/humins	HCl	$k_i C_H^+ C_{Fru}$	129 ± 10	−4.92 ± 0.19[b]	15.5	26, 27
Glucose → HMF	HCl	$k_i (C_H^+)^{1.29} C_{Glu}$	160 ± 5		18.4 ± 1.0[d]	28
Glucose → humins	HCl	$k_i [0.29 + (C_H^+)^{2.76}] C_{Glu}$	51 ± 2		3.9 ± 0.5[d]	28

[a] Reverse reactions modeled based on literature equilibrium constants.[11,30] [b] Reference temperature of 381 K used for these parameters.[27] [c] Units of A_0 expressed in min^{-1}. [d] Units of A_0 expressed in M^{-n} min^{-1}, where n is the exponent associated with C_H^+.

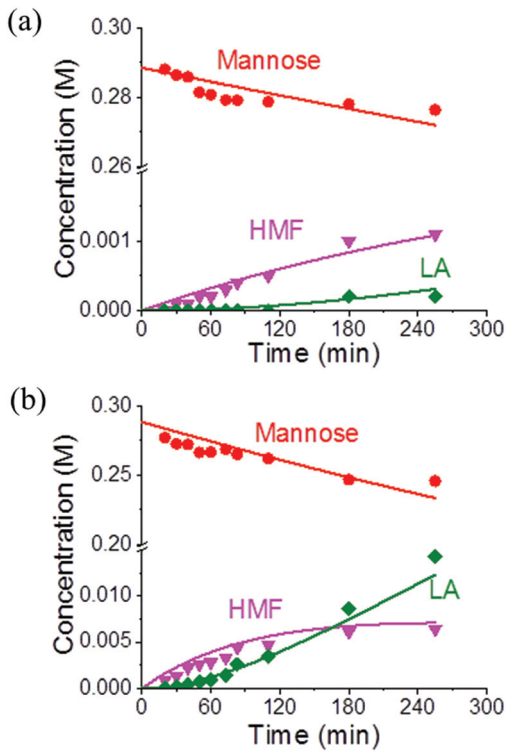

Fig. 1 Concentration profiles of 5 wt% mannose dehydration in aqueous HCl (45 mM, pH = 1.35) at 110 °C (a) and 130 °C (b) from experiments 7 and 8 in Table 1. Measurable compounds include mannose (circles), HMF (triangles), LA (diamonds), and FA (not shown).

catalyzed HMF rehydration to FA/LA and HMF degradation to humins are similar,[7] so the change in selectivity of the HMF consumption paths with temperature underscores that there is a Lewis acid-catalyzed path of humin formation from HMF. This finding is corroborated by the fact that FA forms in excess of LA, especially at lower temperatures (see ESI Fig. S1†), where the Lewis acid chemistry is dominant. This situation differs from typical Brønsted acid rehydration chemistry that produces an equimolar amount of FA and LA.[26] Given the high yield to humins, we hypothesize that FA is mainly produced as a byproduct of HMF condensation leading to humins *via* a Lewis-acid catalyzed path. This is reminiscent of the additional retro-aldol path in glucose dehydration in HCl.[9] The Lewis acid catalyzed reaction network (shown with dotted lines in Scheme 1) accounts for this finding.

Sugar isomerization and epimerization reactions in $CrCl_3$

Typical concentration profiles in aqueous $CrCl_3$ starting from glucose and fructose are shown in Fig. 3a and b, respectively. Glucose primarily isomerizes to fructose at short times. As the reaction proceeds, fructose dehydrates to HMF, which further rehydrates to LA and FA. Humins also form. In order to rationalize the formation of HMF, LA, and FA, which are considered as Brønsted acid-catalyzed products, we previously showed, using the speciation model,[14] that hydrolysis of the hydrated $Cr(H_2O)_6^{3+}$ ion

$$Cr(H_2O)_6^{3+} + H_2O \Leftrightarrow Cr(H_2O)_5OH^{2+} + H_3O^+$$

decreases the pH. The reaction shown above, and other similar ones, is sufficient to drop the pH of the solution to ~1.7 at reaction conditions, leading to Brønsted acid-catalyzed chemistry.

It is now well established that homogeneous Brønsted acids, such as HCl, decrease the reactivity of $CrCl_3$ in glucose–fructose isomerization based on reversing the hydrolysis reaction (shown above).[14,23] To explain this phenomenon, we proposed that the ionic species $Cr(H_2O)_5OH^{2+}$ is the active species for the isomerization and the addition of HCl shifts the hydro-

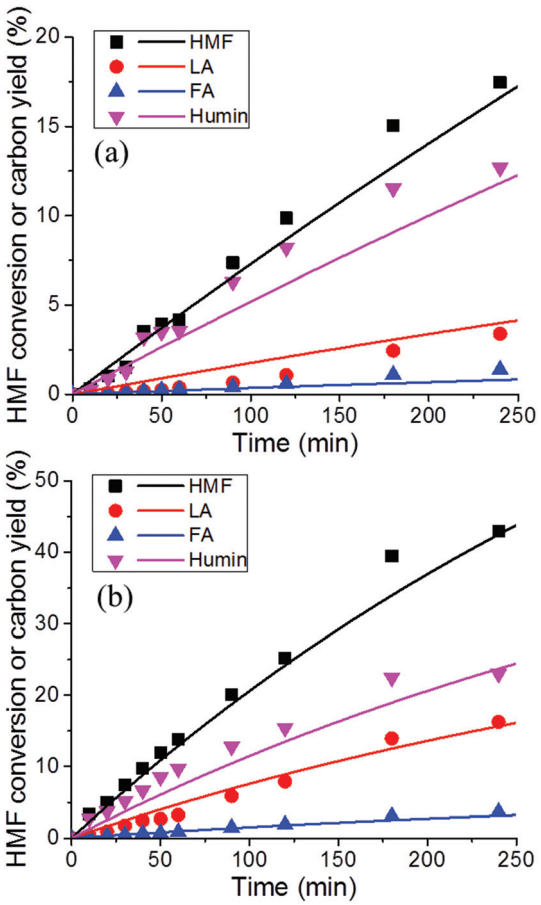

Fig. 2 HMF conversion and carbon yield of products at (a) 110 °C and (b) 130 °C in the presence of 5 mM aqueous $CrCl_3$. Data (points) from experiments 5 and 6 in Table 1. Lines represent model predictions.

lysis reaction reducing the concentration of the active centers.[14] Consistent with the earlier results, Mushrif *et al.* showed that $Cr(H_2O)_5OH^{2+}$ catalyzes glucose–fructose isomerization more effectively than $Cr(H_2O)_6^{3+}$ using first-principles molecular dynamics simulations.[33,34] These findings are consistent with HCl reducing $CrCl_3$ activity, since based on the speciation distribution of $CrCl_3{\cdot}6H_2O$ in aqueous solutions the $Cr(H_2O)_5OH^{2+}$ ion is most abundant between pH 2–4 at 100 °C.[35,36]

In addition to the effect of Brønsted acids on the rate of Lewis acid-catalyzed sugar isomerization, Lewis acid catalysts also affect the rate of fructose dehydration and HMF degradation indirectly by promoting new paths leading to humins (Table 2). Aside from these negative couplings between Lewis and Brønsted acid catalysts, the one-pot reactor drives the equilibrium-limited glucose–fructose isomerization to high conversions *via* dehydrating fructose to HMF thus overcoming the otherwise very slow glucose dehydration to HMF *via* Brønsted acid-catalyzed chemistry alone. Given these tradeoffs, understanding the effect of interplay of the two catalysts on HMF yield and rate is important to determine the optimal catalyst concentrations.

In attempting to correlate the glucose consumption rate with the active species concentration over a wide pH range, we found that the change in $Cr(H_2O)_5OH^{2+}$ concentration is significantly greater than the change in the reaction rate (not shown). Indeed, Choudhary *et al.* concluded that $Cr(H_2O)_5OH^{2+}$ must be the active species based on kinetics measurements mainly without HCl (and a single experiment when 0.1 M HCl was added).[14] The OLI speciation model relies on thermodynamic parameters determined in aqueous solution at higher pH.[36–39] Formation of oligomers is expected at low pH that are not accounted for.[40] To overcome these limitations, we employ an empirical representation for the activity of the catalytically active Lewis acid species:

$$a_L = \left(\frac{[CrOH^{2+}]}{[H^+]}\right)^{1/3} \quad (1)$$

The concentrations of the species are determined using the OLI software. The exponent in eqn (1) was determined by regressing data of experiments 1–6 and 9–16 in Table 1. Fig. S2† shows the predicted value of a_L for experiments 9 and 19–22 in Table 1. The functional form of a_L captures well the change in apparent rate constant, considering experiments 19–22 were not used to determine the exponent in eqn (1).

Fig. 3b shows the concentration profiles when fructose is the substrate. The major product of this reaction is HMF, followed by LA and FA, formed from Brønsted acid-catalyzed dehydration whereas the glucose and mannose concentrations

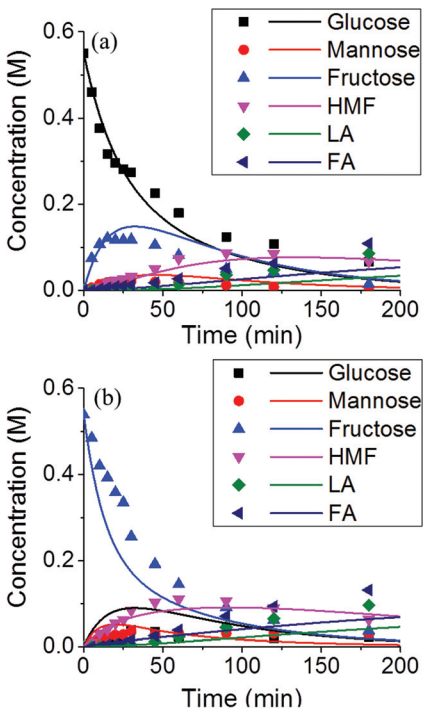

Fig. 3 Representative concentration profiles starting with (a) 10 wt% glucose and (b) 10 wt% fructose in 17 mM $CrCl_3$ at 140 °C taken from ref. 14 (experiments 11 and 13 in Table 1). Lines represent predicted concentration profiles.

are low. The $CrCl_3$-induced Brønsted acidity is therefore strong enough that the fructose dehydration is faster than the Lewis acid-isomerization to glucose.

The hexose sugars may follow two different isomerization paths catalyzed by Lewis acids. First glucose can convert to fructose and fructose to mannose *via* an intramolecular hydride transfer between C1 to C2.[41,42] Glucose may also convert directly to mannose *via* the Bilik mechanism through a 1 and 2 intramolecular carbon shift.[42,43] Fig. 3 shows that fructose produces glucose and mannose in similar molar amounts after five minutes, indicating that both intramolecular hydride transfer pathways are active in solution. On the other hand, glucose produces fructose with much higher selectivity than mannose, indicating that intrahydride transfer dominates over Bilik reaction. This finding is consistent with prior work using Sn-BEA for glucose chemistry.[43] Rajabbeigi *et al.* also found that glucose conversion to mannose is an order of magnitude slower than glucose–fructose isomerization and fructose–mannose isomerization.[30] Glucose, fructose, and mannose may all also degrade to humins. Therefore, we can conclude that our data are in agreement and support the reaction network shown with dashed arrows in Scheme 1.

The activation energies of glucose–fructose and fructose–mannose isomerization are similar, which may be expected given that both reactions proceed *via* the same mechanism of 1,2 intramolecular hydride transfer. Our reported value is in excellent agreement with the first-principles predicted value of 104 kJ mol^{-1}.[33] In comparison to solid Lewis acid catalysts, Sn-BEA has a similar activation energy (95 kJ mol^{-1})[30] whereas Ti-BEA has a higher value (155 kJ mol^{-1}).[13] The activation energy reported here for glucose–fructose isomerization differs from that reported by Choudhary *et al.*[14] (64 kJ mol^{-1}) because Table 2 includes the contribution of changing speciation equilibria with temperature and also considers a wider dataset.

When HCl is added to aqueous $CrCl_3$ solution, Brønsted acid catalyzed reactions become more prevalent. It is therefore important to understand the relative rates of $CrCl_3$- and HCl-catalyzed reactions, particularly how the rate of glucose isomerization compares to that of fructose dehydration. At 130 °C with 5 mM $CrCl_3$, the apparent rate constant of glucose isomerization to fructose of 0.01 min^{-1} is higher than that of fructose dehydration to HMF of 0.0022 min^{-1} (estimated considering the predicted pH = 2.3 of $CrCl_3$ solution) by fivefold.

Effects of $CrCl_3$ concentration and temperature on rate and yields

Fig. 4 shows the experimentally observed glucose conversion, fructose yield, and HMF yield as a function of time at different catalyst concentrations. The glucose consumption rate increases with increasing $CrCl_3$ concentration. Recently, Jia *et al.* found that the yields of fructose and HMF as a function of glucose conversion do not change with catalyst concentration at 110 °C.[20] Our data at higher temperatures (Fig. 4b and c) also support this finding since fructose and HMF yields are not sensitive to changes in the catalyst concentration at the same glucose conversion. These findings indicate that the relative rates of desirable (isomerization and dehydration) and undesirable (humin formation) reactions have weak dependence on $CrCl_3$ concentration. So the enhancement in glucose conversion rate must be balanced by similar enhancement in the other reactions. This trend is consistent with each $CrCl_3$-catalyzed reaction having the same functional dependence on $CrCl_3$ concentration and potentially involving the same catalytically active species. The a_L term in Table 2 reflects these observations, since it does not change for different reactions (the model captures this well; see Fig. S4†).

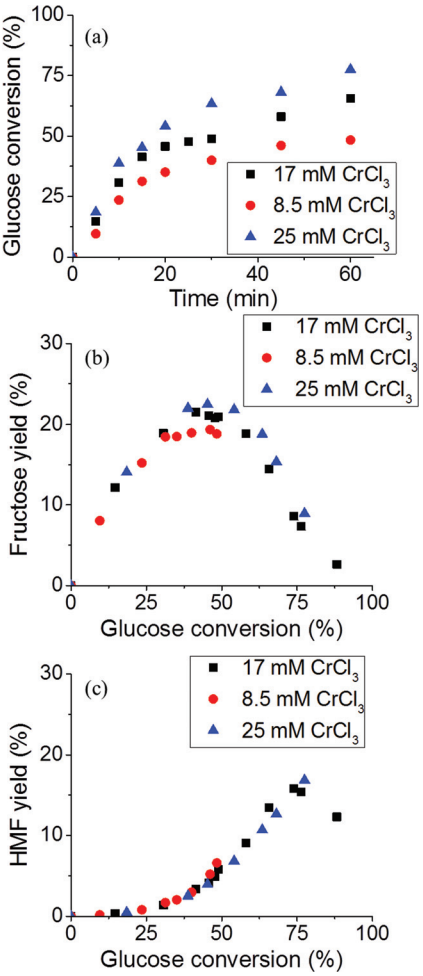

Fig. 4 (a) Glucose conversion as a function of time, and yield of (b) fructose and (c) HMF as a function of glucose conversion at 140 °C at three different $CrCl_3$ concentrations. Data from experiments 23 and 24 in Table 1.

Fig. 5 shows that the yields of fructose, HMF and humins do not vary with reaction temperature at the same glucose conversion. While the absolute rate of glucose conversion increases with increasing temperature over the range of 110–150 °C, the relative rates of isomerization and degradation reactions do not change consistent with the observation of Jia *et al.* at 90–130 °C.[20] The temperature insensitivity of the yield suggests that the activation energies of the most important reactions have similar values. These important reactions

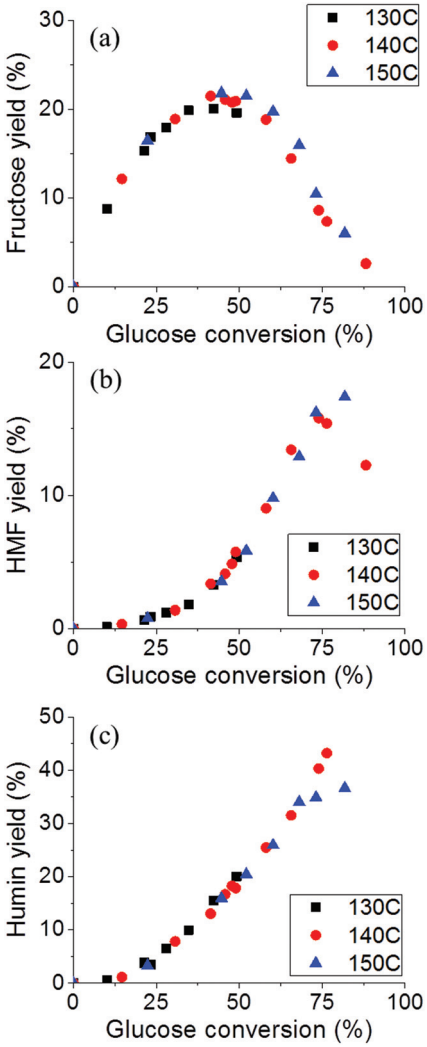

Fig. 5 (a) Fructose yield, (b) HMF yield, and (c) humin carbon yield at different temperatures *vs.* glucose conversion. Experiments 12–14 in Table 1.

include glucose–fructose isomerization, fructose dehydration to HMF, and humin-formation reactions. We determine the most important of these degradation reactions by examining the predicted sources of the humins (Fig. 6). Fig. 6 shows that most of the humins form from either fructose (>50% from Lewis acid-catalyzed reactions) or glucose (25–40% from Lewis acid-catalyzed reactions). These reactions have comparable activation energies (127 *vs.* 114 kJ mol^{-1}), and thus, as the temperature changes, the rates of fructose degradation to humins and fructose dehydration to HMF vary proportionally. This rationalizes the temperature-insensitivity of fructose and HMF yield in $CrCl_3$ as shown in Fig. 5 (see Fig. S5† for model predictions). These findings also agree with earlier work by Weingarten *et al.*, who determined that increasing the number of Lewis acid sites increases the formation of humins from glucose,[44] and highlight the importance of reducing the Lewis acid-catalyzed humin formation reactions of sugars, particularly of fructose.

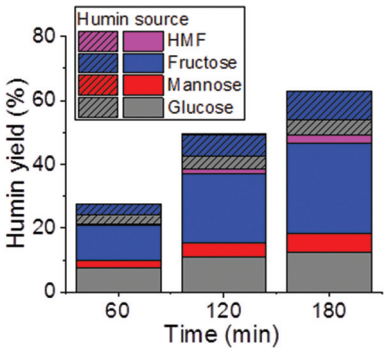

Fig. 6 Humins yield after 1, 2, and 3 h of reaction (10 wt% glucose, 130 °C, 5 mM $CrCl_3$) broken down by source. Hashes indicate Brønsted acid-catalyzed reactions; un-hashed bars indicate Lewis acid-catalyzed reactions.

Taken together, these findings indicate that varying the concentration of $CrCl_3$ or adjusting the temperature are not effective strategies for improving HMF yield from glucose, a key factor in improving the economic viability of this process.[45] Therefore, below we evaluate the possibility of improving HMF yield by adding HCl to $CrCl_3$ in aqueous solution.

Optimizing HMF yield in tandem reactions

Unlike temperature and $CrCl_3$ concentration, adding HCl to a reactor does change HMF yield from glucose (Fig. S6†) by simultaneously increasing the rate of fructose dehydration and decreasing the rate of glucose isomerization. The additional HCl would be beneficial if faster fructose dehydration improved HMF selectivity more than the reduced glucose isomerization hurt it. In order to understand which reactions control the HMF rate, Fig. 7 shows the normalized sensitivity coefficient (NSC) of HMF selectivity to changes in the rate constants of all reactions when only $CrCl_3$ is present. Since the NSC of fructose dehydration to HMF is higher than that of

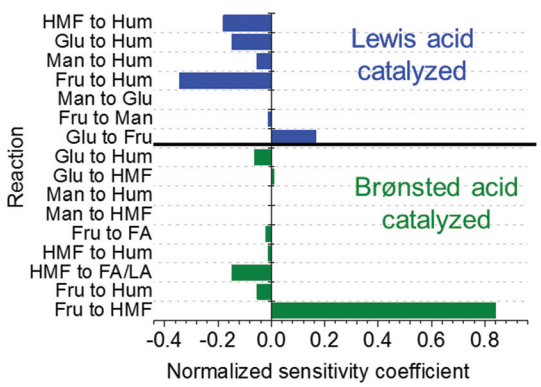

Fig. 7 Normalized sensitivity coefficient of HMF selectivity after 5 h to rate constants of each reaction at 130 °C with 5 mM $CrCl_3$.

glucose–fructose isomerization, adjusting the HCl concentration should have the most pronounced impact on HMF selectivity. However, these sensitivities may change as the amount of HCl in the system increases.

Recently, Patet *et al.* explored *para*-xylene production from dimethylfuran and ethylene, a tandem reaction involving a homogeneous Diels–Alder cycloaddition followed by a Brønsted acid catalyzed dehydration.[46] They observed a clear kinetic regime change upon increasing the amount of Brønsted acid catalyst. At low catalyst concentrations the rate increases with increasing catalyst concentration and eventually plateaus at high catalyst concentrations, accompanied with a change in the rate-limiting step from Brønsted-acid catalyzed to the uncatalyzed Diels–Alder reaction. Similar trends have been observed in forthcoming work studying glucose conversion to HMF using a bifunctional H-BEA catalyst.[47] Like other tandem reactions, a change in kinetic regimes is observed herein as the HCl concentration increases (Fig. 8a), accompanied by a change in the rate-limiting step (Fig. 8b). When the HCl concentration is low Brønsted catalyzed dehydration is the rate limiting step. The opposite can be concluded in the case of solution with high HCl concetrations. The maximum of the HMF reaction rate instead of the plateau arises from the enhancement of the HMF degradation reactions at high Brønsted acid catalyst concentrations, while such degradation reactions in the case of *para*-xylene example were slow. These results show that one needs to balance the Lewis acid and Brønsted acid concentrations to optimize HMF yield and rate.

Given the nonlinear dependence of HMF yield on HCl concentration and in order to understand the interplay of the two catalysts, we performed parametric studies. Fig. 9 shows the maximum HMF yield and the corresponding time as a function of HCl concentration at fixed $CrCl_3$ concentration (full profiles of conversion and yield for select HCl concentrations are given in Fig. S7†). When more $CrCl_3$ is present, the optimal HMF yield occurs at higher HCl concentration but the maximum HMF yield itself does not change. Interestingly, a volcano relationship with an optimum HCl concentration for each $CrCl_3$ concentration is observed, reflecting a change in the rate-limiting step from dehydration at low HCl concentrations to isomerization at high HCl concentrations (sensitivity analysis shown in Fig. 8b). As shown in Fig. 9a, HMF yield is maximized when HCl concentration is ~0.02 M, where the NSC of isomerization and dehydration reactions are similar (Fig. 8b), indicating the desirability of balancing isomerization and dehydration. Generally, lower pH decreases processing time, so intermediate concentrations of HCl can both increase HMF yield and decrease the time it takes to reach that yield.

In order to assess the model prediction, we conducted additional experiments. Fig. 10 compares experimental data (symbols) and model predictions (lines) of glucose conversion and HMF yield as a function of time for three HCl concentrations. While the glucose conversion is not captured

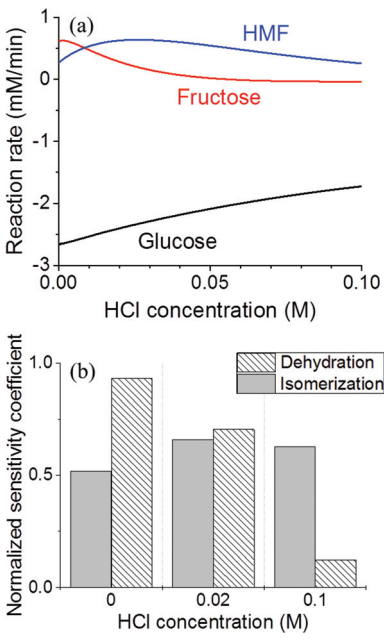

Fig. 8 (a) Predicted reaction rates of glucose, fructose, and HMF as a function of HCl concentration and (b) normalized sensitivity coefficient of HMF reaction rate at different HCl concentration after 1 hour of reaction. Conditions: 10 wt% glucose, 5 mM $CrCl_3$, 130 °C.

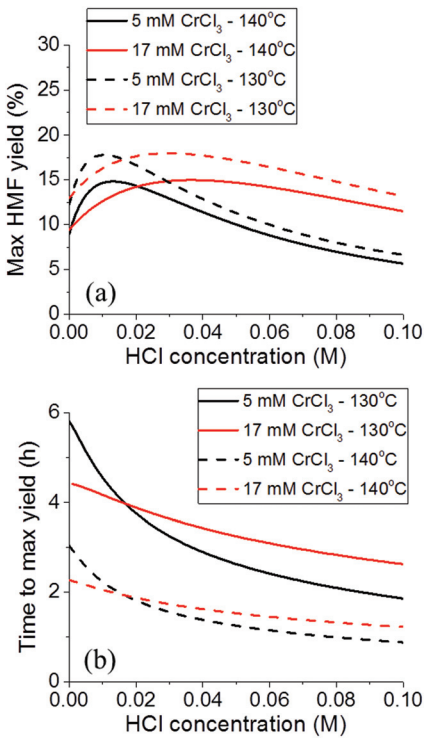

Fig. 9 (a) Maximum HMF yield and (b) time to reach the maximum yield as a function of HCl concentration at different Lewis acid catalyst concentrations and temperatures.

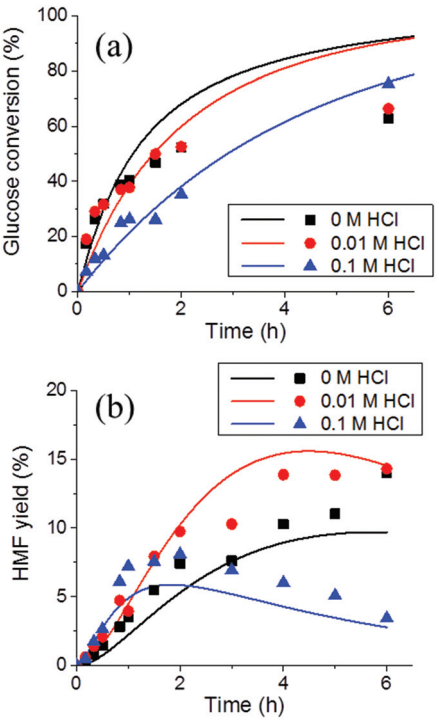

Fig. 10 Experimentally observed (symbols) and model predictions (lines) (a) glucose conversion and (b) HMF yield in aqueous $CrCl_3$ + HCl at 5 wt% glucose and 130 °C with 5 mM $CrCl_3$ for various HCl concentrations indicated. Experiments 25 and 26 in Table 1.

as well at long times, the HMF yield is predicted very well and underscores the non-monotonic dependence of HMF yield on HCl concentration. This is the first model-based prediction indicating that there are optimal catalyst concentrations.

Reactive extraction

A disadvantage of high Brønsted acidity is that in addition to enhancing fructose dehydration rate it also enhances the rates of HMF degradation reactions. The addition of an organic extracting phase can reduce HMF degradation products[48] and was shown to work for this tandem reaction.[14] Fig. 11 shows the predicted concentration profile for this biphasic system compared to experimental data for a reactor with a 2 : 1 volume ratio of THF : H_2O and for an infinite partition coefficient (ideal extraction, shown in dashed line). While glucose conversion and fructose yield are well-predicted, the HMF yield is somewhat under-estimated. Wrigstedt *et al.* found that fructose in aqueous $CrCl_3$/HCl reacts differently in the presence of different inorganic salts, such as NaCl and KCl.[23] We hypothesize that the underestimation could be due to salt effects not captured by the model. Importantly, extraction significantly enhances the HMF yield. Furthermore, even in the presence of an extractant, the HMF yield is maximized at moderate HCl concentrations (Fig. S8†).

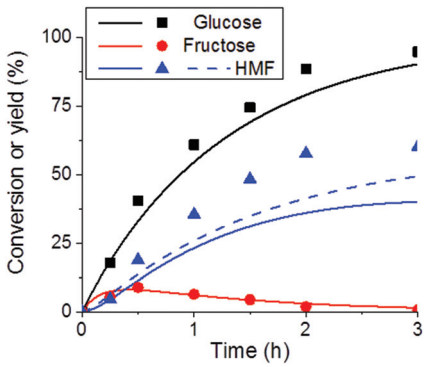

Fig. 11 Predicted and experimental glucose conversion, fructose yield, and HMF yield as a function of time in a biphasic reactor with 2 : 1 volume ratio of THF (partition coefficient = 7, shown by solid lines) and ideal extractant (dashed lines). Experimental conditions given in Experiment 27 in Table 1.

Conclusions

We have conducted select experiments in order to develop and assess the first-of its kind model describing the tandem conversion of glucose to HMF through fructose in aqueous $CrCl_3$–HCl. Experimental data indicate that glucose converts to fructose and fructose converts to mannose mainly *via* 1,2 intrahydride transfer, whereas epimerization (Bilik) reaction *via* intracarbon shift is considerably slow under our conditions, consistent with the mechanism over Sn-BEA zeolite of the Davis group[43] and in support of the NMR data on the glucose to fructose isomerization over $CrCl_3$ catalyst of our prior work.[16] Brønsted-acid catalysis of mannose leads primarily to humins, and HMF in $CrCl_3$ undergoes considerable loss to humins and formic acid especially at low temperatures. Consistent with recent work,[20] we find that increasing temperature and $CrCl_3$ concentration do not change either fructose or HMF yield at constant glucose conversion and are not effective for HMF yield optimization.

In agreement with our previous work,[14] we show that Lewis acid metal salts interact with the homogeneous Brønsted acids in complex ways. Specifically, hydrolysis of the hydrated Cr^{3+} releases protons and drives endogenous Brønsted acid chemistry. Exogenous Brønsted acids retard the rate of isomerization due to changing the speciation (reducing the active species concentration) but at the same time increase the rate of fructose dehydration and HMF degradation. In turn, Lewis acid salts accelerate the rate of glucose conversion to fructose mainly *via* isomerization but also open up new channels, mainly Lewis-catalyzed humin formation from sugars (fructose > glucose > mannose) and to less extent from HMF, which reduce HMF yield. Finally, the coupling of Lewis and Brønsted acids in a single pot overcomes equilibrium limitations of the glucose–fructose isomerization leading to high glucose conversions. Model predictions and assessment experiments clearly show for the first time that the interplay of these complex interactions leads to HMF yield being maximized at moderate

HCl concentrations for each $CrCl_3$ concentration. This volcano-like behavior is accompanied with a change in the rate-limiting step from fructose dehydration to glucose isomerization as the concentration of the Brønsted acid increases. The maximum HMF yield in a single aqueous phase is only modest and appears independent of catalysts' concentrations as long as they are appropriately balanced. Finally, experiments and modeling indicate significant increase in yield using a biphasic system. Fundamentally, as the concentration of the Brønsted acid increases, a change in kinetic regimes in the reaction rate of HMF production is predicted, consistent with recent studies in other tandem reactions catalyzed by different catalysts, underscoring that this is a generic behavior of cascade reactions.

Acknowledgements

The authors would like to thank Dr Marta León, who conducted Experiments 17 and 18. This work was supported as part of the Catalysis Center for Energy Innovation, an Energy Frontier Research Center funded by the US Dept. of Energy, Office of Science, Office of Basic Energy Sciences under award number DE-SC0001004.

References

1 J. E. Holladay, J. F. White, J. J. Bozell and D. K. Johnson, *Top Value-Added Chemicals from Biomass - Volume II—Results of Screening for Potential Candidates from Biorefinery Lignin*, 2007.
2 Y. Román-Leshkov, C. J. Barrett, Z. Y. Liu and J. A. Dumesic, *Nature*, 2007, **447**, 982–985.
3 B. Saha and M. M. Abu-Omar, *ChemSusChem*, 2015, **8**, 1133–1142.
4 C. L. Williams, C.-C. Chang, P. T. Do, N. Nikbin, S. Caratzoulas, D. G. Vlachos, R. F. Lobo, W. Fan and P. J. Dauenhauer, *ACS Catal.*, 2012, **2**, 935–939.
5 P. Azadi, R. Carrasquillo-Flores, Y. J. Pagán-Torres, E. I. Gürbüz, R. Farnood and J. A. Dumesic, *Green Chem.*, 2012, **14**, 1573–1576.
6 Z. Lin, M. G. Ierapetritou and V. Nikolakis, *AIChE J.*, 2013, **59**, 2079–2087.
7 R.-J. van Putten, J. C. van der Waal, E. de Jong, C. B. Rasrendra, H. J. Heeres and J. G. deVries, *Chem. Rev.*, 2013, **113**, 1499–1597.
8 R.-J. van Putten, J. N. Soetedjo, E. A. Pidko, J. C. van der Waal, E. J. Hensen, E. de Jong and H. J. Heeres, *ChemSusChem*, 2013, **6**, 1681–1687.
9 L. Yang, G. Tsilomelekis, S. Caratzoulas and D. G. Vlachos, *ChemSusChem*, 2015, **8**, 1334–1341.
10 R. DiCosimo, J. McAuliffe, A. J. Poulose and G. Bohlmann, *Chem. Soc. Rev.*, 2013, **42**, 6437–6474.
11 R. N. Goldberg and Y. B. Tewari, *J. Phys. Chem. Ref. Data*, 1995, **24**, 1765–1801.
12 S. P. Simeonov, J. A. S. Coelho and C. A. M. Afonso, *ChemSusChem*, 2013, **6**, 997–1000.
13 R. Bermejo-Deval, R. S. Assary, E. Nikolla, M. Moliner, Y. Román-Leshkov, S.-J. Hwang, A. Palsdottir, D. Silverman, R. F. Lobo, L. A. Curtiss, *et al.*, *Proc. Natl. Acad. Sci. U. S. A.*, 2012, **109**, 9727–9732.
14 V. Choudhary, S. H. Mushrif, C. Ho, A. Anderko, V. Nikolakis, N. S. Marinkovic, A. I. Frenkel, S. I. Sandler and D. G. Vlachos, *J. Am. Chem. Soc.*, 2013, **135**, 3997–4006.
15 E. Nikolla, Y. Román-Leshkov, M. Moliner and M. E. Davis, *ACS Catal.*, 2011, **1**, 408–410.
16 S. Caratzoulas, M. E. Davis, R. J. Gorte, R. Gounder, R. F. Lobo, V. Nikolakis, S. I. Sandler, M. A. Snyder, M. Tsapatsis and D. G. Vlachos, *J. Phys. Chem. C*, 2014, **118**, 22815–22833.
17 R. Otomo, T. Yokoi, J. N. Kondo and T. Tatsumi, *Appl. Catal., A*, 2014, **470**, 318–326.
18 M. G. Mazzotta, D. Gupta, B. Saha, A. K. Patra, A. Bhaumik and M. M. Abu-Omar, *ChemSusChem*, 2014, **7**, 2342–2350.
19 B. Saha and M. M. Abu-Omar, *Green Chem.*, 2014, **16**, 24–38.
20 S. Jia, K. Liu, Z. Xu, P. Yan, W. Xu, X. Liu and Z. C. Zhang, *Catal. Today*, 2014, **234**, 83–90.
21 C. B. Rasrendra, J. N. Soetedjo, I. Makertihartha, S. Adisasmito and H. J. Heeres, *Top. Catal.*, 2012, **55**, 543–549.
22 C. Loerbroks, J. van Rijn, M.-P. Ruby, Q. Tong, F. Schüth and W. Thiel, *Chem. – Eur. J.*, 2014, **20**, 12298–12309.
23 P. Wrigstedt, J. Keskiväli, M. Leskelä and T. Repo, *ChemCatChem*, 2015, **7**, 501–507.
24 Y. J. Pagán-Torres, T. Wang, J. M. R. Gallo, B. H. Shanks and J. A. Dumesic, *ACS Catal.*, 2012, **2**, 930–934.
25 O. Casanova, S. Iborra and A. Corma, *J. Catal.*, 2010, **275**, 236–242.
26 T. D. Swift, C. Bagia, V. Choudhary, G. Peklaris, V. Nikolakis and D. G. Vlachos, *ACS Catal.*, 2014, **4**, 259–267.
27 T. D. Swift, C. Bagia, V. Choudhary, G. Peklaris, V. Nikolakis and D. G. Vlachos, *ACS Catal.*, 2014, **4**, 1320–1320.
28 R. Weingarten, J. Cho, R. Xing, W. C. Conner and G. W. Huber, *ChemSusChem*, 2012, **5**, 1280–1290.
29 M. Moliner, Y. Román-Leshkov and M. E. Davis, *Proc. Natl. Acad. Sci. U. S. A.*, 2010, **107**, 6164–6168.
30 N. Rajabbeigi, A. I. Torres, C. M. Lew, B. Elyassi, L. Ren, Z. Wang, H. Je Cho, W. Fan, P. Daoutidis and M. Tsapatsis, *Chem. Eng. Sci.*, 2014, **116**, 235–242.
31 P. Wang, A. Anderko and R. D. Young, *Fluid Phase Equilib.*, 2002, **203**, 141–176.
32 B. Girisuta, L. P. Janssen and H. J. Heeres, *Chem. Eng. Res. Des.*, 2006, **84**, 339–349.
33 S. H. Mushrif, J. J. Varghese and D. G. Vlachos, *Phys. Chem. Chem. Phys.*, 2014, **16**, 19564–19572.
34 S. H. Mushrif, J. J. Varghese and C. B. Krishnamurthy, *Phys. Chem. Chem. Phys.*, 2015, **17**, 4961–4969.

35 B. Beverskog and I. Puigdomenesch, *Corros. Sci.*, 1997, **39**, 43–57.
36 E. L. Shock and H. C. Helgeson, *Geochim. Cosmochim. Acta*, 1988, **52**, 2009–2036.
37 E. H. Oelkers, H. C. Helgeson, E. L. Shock, D. A. Sverjensky, J. W. Johnson and V. A. Pokrovskii, *J. Phys. Chem. Ref. Data*, 1995, **24**, 1401–1560.
38 V. A. Pokrovskii and H. C. Helgeson, *Am. J. Sci.*, 1995, **295**, 1255–1342.
39 E. L. Shock, D. C. Sassani, M. Willis and D. A. Sverjensky, *Geochim. Cosmochim. Acta*, 1997, **61**, 907–950.
40 D. Rai, B. M. Sass and D. A. Moore, *Inorg. Chem.*, 1987, **26**, 345–349.
41 Y. Román-Leshkov, M. Moliner, J. A. Labinger and M. E. Davis, *Angew. Chem., Int. Ed.*, 2010, **49**, 8954–8957.
42 R. Bermejo-Deval, R. Gounder and M. E. Davis, *ACS Catal.*, 2012, **2**, 2705–2713.
43 R. Bermejo-Deval, M. Orazov, R. Gounder, S.-J. Hwang and M. E. Davis, *ACS Catal.*, 2014, **4**, 2288–2297.
44 R. Weingarten, Y. T. Kim, G. A. Tompsett, A. Fernández, K. S. Han, E. W. Hagaman, W. C. Conner, J. A. Dumesic and G. W. Huber, *J. Catal.*, 2013, **304**, 123–134.
45 Z. Lin, V. Nikolakis and M. G. Ierapetritou, *Ind. Eng. Chem. Res.*, 2015, **54**, 2366–2378.
46 R. E. Patet, N. Nikbin, C. L. Williams, S. K. Green, C.-C. Chang, W. Fan, S. Caratzoulas, P. J. Dauenhauer and D. G. Vlachos, *ACS Catal.*, 2015, **5**, 2367–2375.
47 T. D. Swift, H. Nguyen, Z. Erdman, J. S. Kruger, V. Nikolakis and D. G. Vlachos, *J. Catal.*, submitted.
48 Y. Román-Leshkov, J. N. Chheda and J. A. Dumesic, *Science*, 2006, **312**, 1933–1937.